Clay Minerals (2024), **59**, 1–10
doi:10.1180/clm.2024.1

CAMBRIDGE UNIVERSITY PRESS

Article

Comparison of the antimicrobial and antioxidant properties of halloysite nanotubes and organoclays as green source materials

Nevin Çankaya[1], Arzu Ünal[2] and Safiye Elif Korcan[1]

[1]Vocational School of Health Services, Usak University, Usak, Türkiye and [2]Faculty of Agriculture, Department of Agricultural, Biotechnology, Iğdır University, Iğdır, Türkiye

Abstract

The antibacterial, antifungal and antioxidant effects of halloysite nanoclay, Cloisite 10A (C10A) and Cloisite 15A (C15A) organonanoclays were examined in this study. The antimicrobial action was assessed using the agar-well method and the disc diffusion method. The free radical-scavenging effects of the clays were determined using the 2,2-diphenyl-1-picrylhydrazyl method. Halloysite showed antimicrobial activity against *Pseudomonas aeruginosa*, *Enterococcus faecalis* and *Staphylococcus aureus*. C10A was effective against both Gram-positive bacteria (*S. aureus*, *Listeria monocytogenes*, *Bacillus subtilis* and *E. faecalis*) and Gram-negative bacteria (*Escherichia coli*, *Klebsiella pneumoniae* and *P. aeruginosa*). Additionally, only C10A was found to have an antimicrobial effect on *Candida glabrata* of 18 mm amongst the tested clays. C15A showed an antimicrobial effect on *S. aureus* and *K. pneumoniae*. It was determined that the antifungal properties of organoclays were higher than those of halloysite. The most effective clay type was determined to be C10A. The positively charged inner surface of the halloysite nanoclay can provide a large area to which negatively charged free radicals can attach. The modified C15A used in this study has two long-chain alkyl groups attached, whereas the modified C10A has a single long-chain alkyl group and a benzyl group attached. It is proposed that the differences in these antimicrobial effects are due to the structures of the molecules. According to these results, organoclays as green source materials could be used as additives and coatings in food processing, biomedical devices, filters and paints due to their antimicrobial and antioxidant properties.

Keywords: Antibacterial; antifungal; antioxidant; halloysite; organoclay

(Received 26 October 2023; revised 2 January 2024; Accepted Manuscript online: 24 January 2024; Associate Editor: Chunhui Zhou)

Halloysite nanotubes (HNTs; $Al_2Si_2O_5(OH)_4{\cdot}nH_2O$) with a hollow tubular morphology (named by mineralogist M. Berthier in 1826) are aluminosilicates of the kaolin group. Recently, experiments have been conducted to create green nanocomposites with antimicrobial activity by incorporating several antimicrobial compounds into HNTs (Massaro *et al.*, 2020). Significant advantages of incorporating HNTs into nanocomposites include improved thermal and mechanical stability of antimicrobial nanocomposites as well as extending their lifespan and release of antimicrobial chemicals (Saadat *et al.*, 2020).

One of the most pressing health issues in the world is microbial infections, which are on the rise as a result of the planet's rapidly increasing human population. These infections have been treated using a number of conventional chemical-based antibacterial agents. The emergence of resistant pathogens, which can result in illnesses that are challenging or impossible to treat, is a key drawback of using such medications. Additionally, the hazardous by-products from making these chemical compounds can cause health issues and pollution of the environment (Haiwei *et al.*, 2016).

Today, studies are being carried out to develop new nanocomposites with antimicrobial properties enhanced with support materials such as HNTs and montmorillonite (MMT; Ding *et al.*, 2014; Duan *et al.*, 2015; Shu *et al.*, 2017; Srivastava & Dwivedi, 2018). Zhao *et al.* (2019) have shown that halloysite has very few side effects on the development of *Caenorhabditis elegans* and that it is only effective on the growth of *C. elegans* offspring. It has been reported that clay nanotubes can be used as a drug to alleviate colitis, as a nanocarrier targeting the inflamed colon by electrostatic adsorption or as an interfacial stabilizer for emulsions (Feng *et al.*, 2023a).

Numerous products and formulations of quaternary ammonium compounds (QACs) are commercially available and widely used in industry. QACs are cationic surfactants (positively charged surfactants) that affect microbial cell walls and membranes. These positively charged compounds show antimicrobial effects by easily binding to the negatively charged surfaces of many microorganisms (Chauret, 2014).

HNTs and organoclays are used in the cosmetics (Kamble *et al.*, 2012) and food industries (Deshmukh *et al.*, 2023; Kumar *et al.*, 2024), as well as in the chemical industry as templates or nanoreactors for biocatalysts (Shchukin *et al.*, 2005) and in the pharmaceutical industry for encapsulation and controlled drug release (Meirelles *et al.*, 2017; Silva *et al.*, 2019). For this reason, scientific studies aimed at expanding and improving these usages by increasing the antimicrobial properties of clays and their derivatives have attracted much recent attention. Liu *et al.* (2023) reported that biocompatible HNT–polymer nanocomposites can be used in drug delivery and are promising

Corresponding author: Nevin Çankaya; Email: nevin.cankaya@usak.edu.tr
Cite this article: Çankaya N, Ünal A, Korcan SE (2024). Comparison of the antimicrobial and antioxidant properties of halloysite nanotubes and organoclays as green source materials. *Clay Minerals* **59**, 1–10. https://doi.org/10.1180/clm.2024.1

Table 1. XRF analysis of the C10A, C15A and HNT clays.

	C10A	C15A	HNT
Loss on ignition (%)	40 ± 2.0	45 ± 2.0	16 ± 2.0
SiO_2 (%)	45 ± 2.0	44 ± 1.0	46 ± 2.0
Al_2O_3 (%)	6.0 ± 1.0	6.0 ± 1.0	37 ± 2.0
Fe_2O_3 (%)	0.5 ± 0.2	0.4 ± 0.2	1.0 ± 0.3
TiO_2 (%)	0.05 ± 0.02	45 ± 2.0	Maximum: 0.30
CaO (%)	1.0 ± 0.1	0.4 ± 0.1	Maximum: 0.15
MgO (%)	1.3 ± 0.2	1.4 ± 0.2	Maximum: 0.45
Na_2O (%)	0.6 ± 0.2	0.6 ± 0.2	Maximum: 0.15
K_2O (%)	1.0 ± 0.1	0.3 ± 0.1	Maximum: 0.45

for other biomedical applications such as tissue engineering, cancer diagnosis/treatment, wound dressing and as biosensors. Therefore, they suggested that the biological effects and toxicology of HNTs should be comprehensively investigated (Liu *et al.*, 2023). Industrial products based on HNTs are developing rapidly due to their good mechanical, thermal and biological properties.

Clay and clay-containing materials can be used in the development of many new industrial products due to their unique mechanical, thermal and biological properties. Because of this, our team has previously conducted physicochemical and mechanical studies of Cloisite 10A (C10A), Cloisite 15A (C15A) and halloysite (Çankaya & Sahın, 2019; Çankaya *et al.*, 2021a, 2021b). In addition, in our studies, it was determined that the anticancer effect of C10A (half-maximal inhibitory concentration (IC_{50}): 3.5 µg mL^{-1}) against HeLa cancer cells was greater than that of halloysite (Çankaya *et al.*, 2021b). Determining the antibacterial, antifungal and antioxidant properties of C10A, C15A and halloysite clays was the goal of the current investigation.

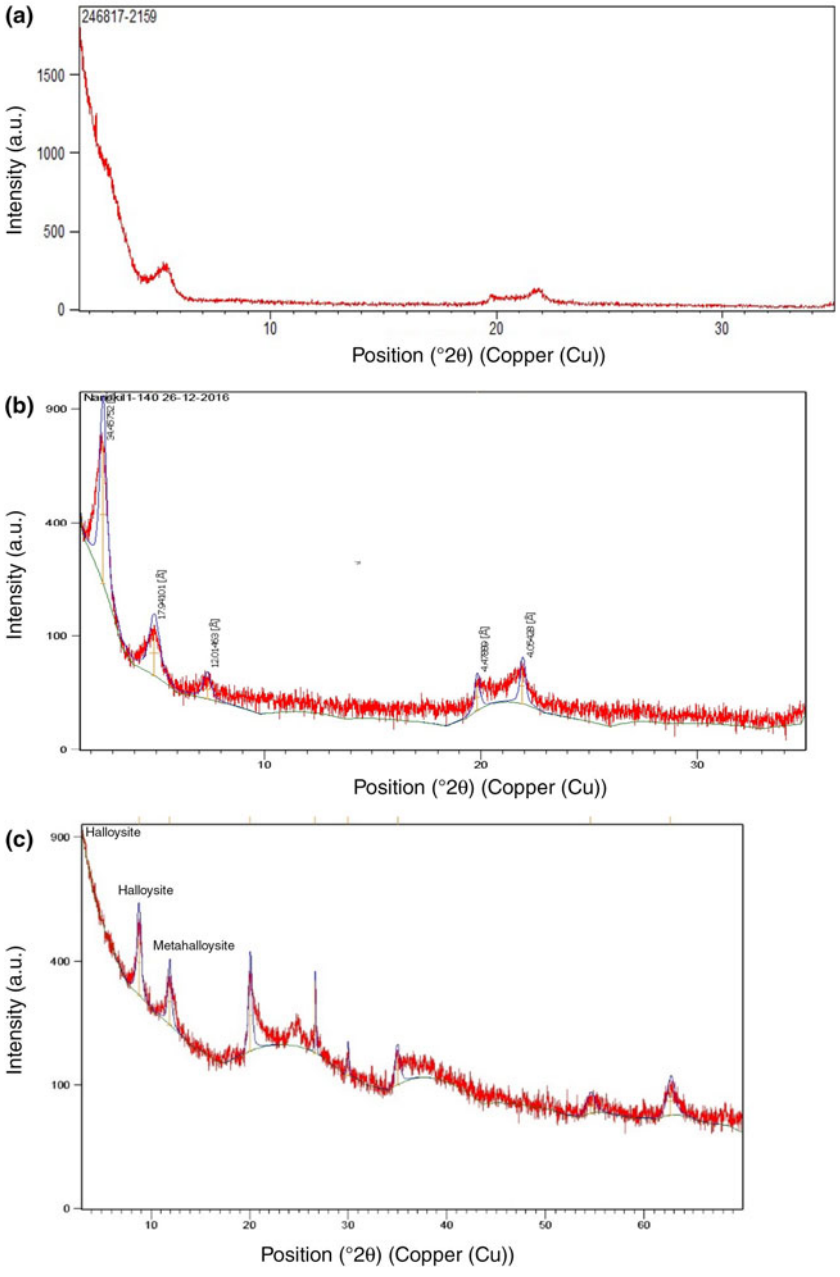

Figure 1. XRD traces of (a) C10A, (b) C15A and (c) halloysite clays.

https://doi.org/10.1180/clm.2024.1 Published online by Cambridge University Press

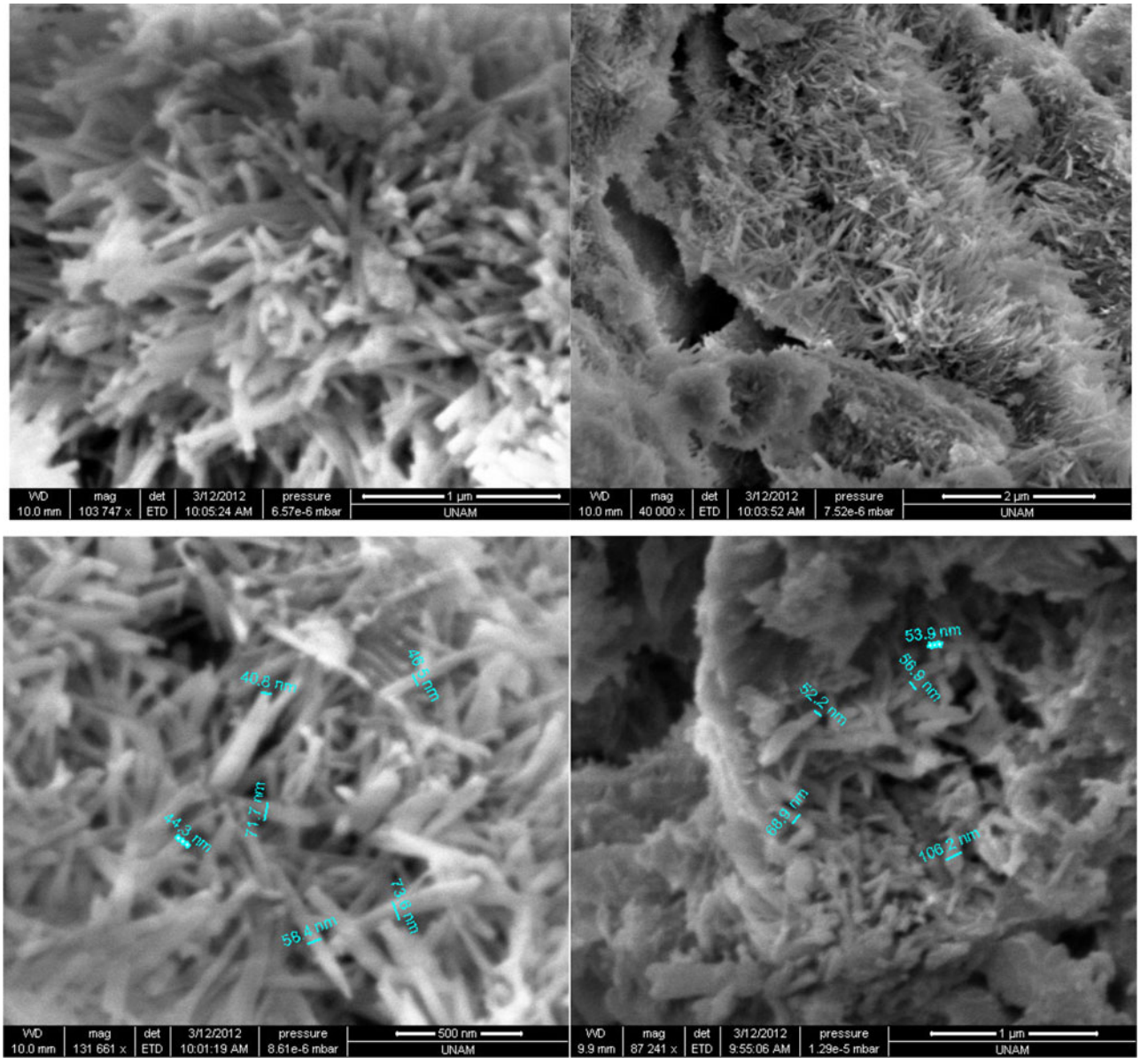

Figure 2. SEM images of HNT.

Experimental

C10A clay (particle size <15 µm; Nanoclay 1-135, modified with dimethyl, benzyl, hydrogenated tallow, quaternary ammonium chloride), C15A organoclay (particle size <20 µm; Nanoclay 1-140, modified with dimethyl, dihydrogenated tallow, quaternary ammonium chloride) and halloysite clay (particle size <10 µm) were purchased from Esan-Eczacıbaşı (Çankaya & Sahın, 2019; Çankaya *et al.*, 2021a). X-ray fluorescence (XRF) chemical analyses of the C10A and C15A organoclays and the HNT clay provided by Esan-Eczacıbaşı are given in Table 1, and their X-ray diffraction (XRD) traces are given in Fig. 1. Although the interlayer distance value of MMT clays is ~15 Å, it can reach 38–40 Å for C10A and C15A when organic modification is performed. Scanning electron microscopy (SEM) and transmission electron microscopy (TEM) images of the HNT clay provided by Esan-Eczacıbaşı are given in Figs 2 & 3. For HNT, the Brunauer–Emmett–Teller (BET) specific surface area is 128 m^2 g^{-1}, maximum moisture is 5.43%, average nanotube length is 1.2 µm, average inner diameter is 20 nm and average outer diameter is 40 nm. The distance between layers is 7 Å for dihydrate and 10 Å for hydrate.

The bacteria (*S. aureus* ATCC 25923, *C. glabrata* ATCC 90030, *B. subtilis* ATCC 6051, *E. faecalis* ATCC 551289, *E. coli* ATCC 25922, *K. pneumoniae* NRLLB4420, *P. aeruginosa* ATCC 27853, *L. monocytogenes* ATCC 1911) and fungi (*Trichoderma longibrachiatum* MK910052.1, *Fusarium solani* KT876631.1, *Mucor plumbeus* MH870585, *Trichoderma viride* MH398583.1, *Neocosmospora falciformis* MH2444 10.1, *Penicillium glabrum* MK910045.1) used in the study were obtained from Usak University Vocational School of Health Services.

Antibacterial and antifungal activity test

The antibacterial effect was assessed using the disc diffusion method. In this study, a qualitative approach was preferred over a quantitative minimum inhibitory concentration (MIC)

https://doi.org/10.1180/clm.2024.1 Published online by Cambridge University Press

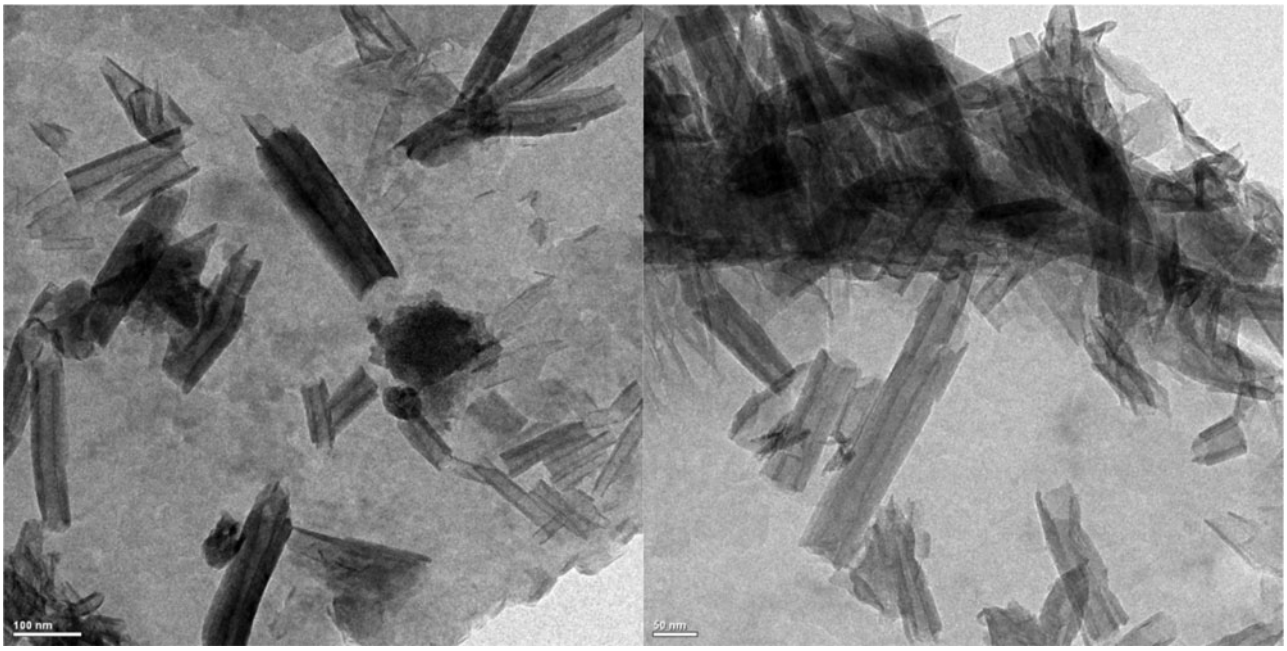

Figure 3. TEM images of HNT.

Table 2. Antimicrobial effect results determined using the disc diffusion method.

Test bacteria	Inhibition zone (mm)								
	Positive control					Negative control	Test materials		
	VA (30 µg)	TE (30 µg)	C (30 µg)	E (15 µg)	P (10 µg)	DMSO	C10A	C15A	Halloysite
S. aureus	21	30	27	30	40	–	27	6	7
C. glabrata	8	19	28	–	7	–	18	–	–
B. subtilis	22	16	36	29	31	–	25	–	–
E. faecalis	22	27	30	12	23	–	27	–	9
E. coli	25	12	30	26	33	–	20	–	–
K. pneumoniae	20	12	25	21	32	–	25	15	–
P. aeruginosa	6	9	12	6	6	–	13	–	10
L. monocytogenes	25	30	32	11	25	–	30	–	–

C = chloramphenicol; E = erythromycin; P = penicillin; TE = tetracycline; VA = vancomycin.

approach as the clay samples were suspended in a broth medium. Briefly, after 0.1 g of C10A, C15A and halloysite clays were dissolved in 1 mL of dimethyl sulfoxide (DMSO), 20 µL of each sample was absorbed into empty antibiotic discs under aseptic conditions. Test strains were incubated for 24 h. The bacterial suspension at 0.5 McFarland turbidity was spread on the Mueller–Hinton agar (MHA) surface with a sterile swab. Paper discs (6 mm) impregnated with halloysite and organoclay were placed on the agar surface. The test solution preparation agent – DMSO – served as a negative control. Petri plates were incubated at 37°C for 24 h. The zone of inhibition around the disc is usually taken as the diameter, which corresponds to the sharpest edge of the region where growth is inhibited from edge to edge and can be measured in millimetres using a calliper. The antimicrobial effect against each test strain was evaluated by comparing C10A, C15A and halloysite inhibition zones with the control inhibition zone (Biemer, 1973; Isik & Özdemir-Kocak, 2009).

To assess antifungal efficacy, the well diffusion method was used. Briefly, 0.1 g of C10A, C15A and halloysite were used in the antifungal activity experiments after they were dissolved in 1 mL of deionized water. Wells of 6 mm were opened in the middle of Petri dishes containing nutrient agar medium, and 20 µL of a sample was inoculated into each well. Then, 20 µL of deionized water was inoculated into the wells as a control to determine whether there was an effect stemming from the sample and solvent. Spot planting of fungal isolates, which were previously defined at the species level *via* molecular analysis, was carried out at equal distances from the well. After 7 days of incubation in the dark at 27 ± 2°C, the distances from the fungal colony to the well were measured. The percentage of inhibition was calculated by comparing these distances with that from the control group (Korcan *et al.*, 2021).

Determination of antioxidant activity using DPPH (free radical-scavenging effect)

The antioxidant activity of the samples was assessed using the 2,2-diphenyl-1-pixyl-hydrazil (DPPH) test, as presented previously (Villano *et al.*, 2007), with some modifications. In brief,

https://doi.org/10.1180/clm.2024.1 Published online by Cambridge University Press

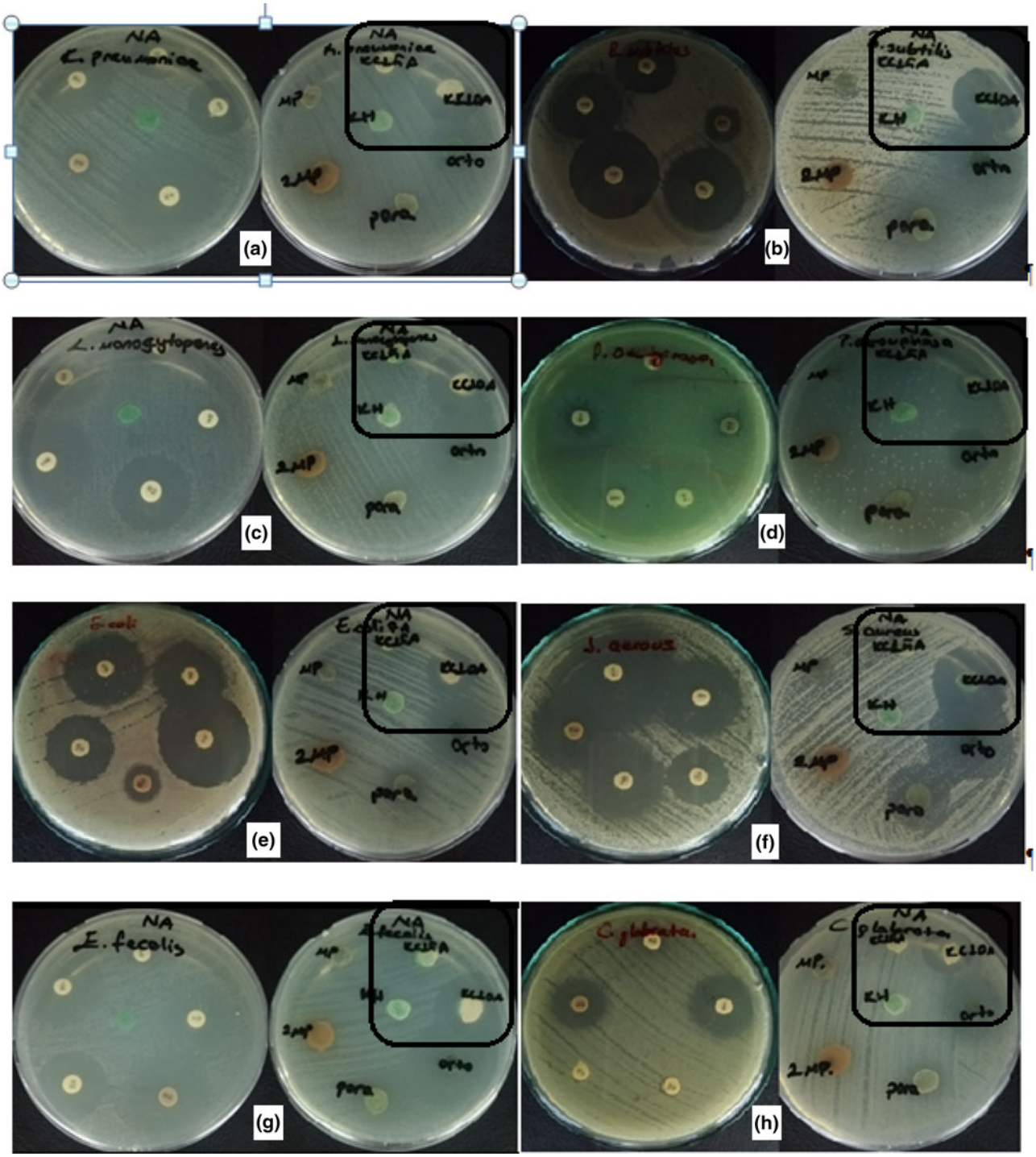

Figure 4. Bacterial inhibition zones formed around clays on agar. (a) *K. pneumoniae*, (b) *B. subtilis*, (c) *L. monocytogenes*, (d) *P. aeruginosa*, (e) *E. coli*, (f) *S. aureus*, (g) *E. faecalis*, (h) *C. glabrata*.

150 µL of each sample was mixed with 5850 µL of DPPH solution. This was then incubated at 27°C for 1 h in the dark. Absorbance was measured at 515 nm with a Shimadzu brand UV-1800 spectrophotometer. The positive control was gallic acid. Equation 1 was used to assess each sample's capacity to scavenge the DPPH radical:

$$\text{Inhibition } (\%) = (A_{\text{control}} - A_{\text{sample}}/A_{\text{control}}) \times 100 \qquad (1)$$

where A_{control} is the absorbance of the control without the sample and A_{sample} is the absorbance of the mixture containing the sample.

Results and discussion

Antibacterial and antifungal activity test results

Table 2 provides the findings obtained regarding the antibacterial effect using the disc diffusion method. C10A appeared to have an

https://doi.org/10.1180/clm.2024.1 Published online by Cambridge University Press

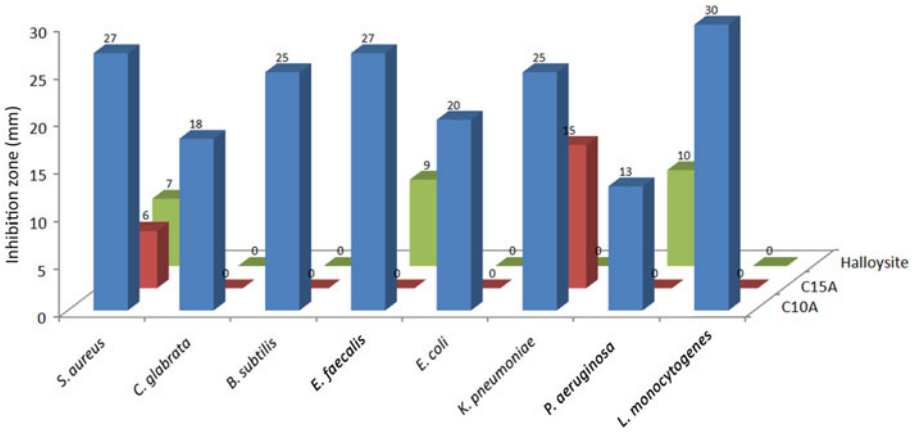

Figure 5. Comparison of the antibacterial properties of the studied clays.

Table 3. Inhibitory effect of the studied clays on fungal mycelium growth.

Test materials	Fungi inhibition (%)					
	T. longibrachiatum	*F. solani*	*M. plumbeus*	*T. viride*	*N. falciformis*	*P. glabrum*
C10A	85.00	17.39	69.41	85.32	25.00	21.68
C15A	40.00	20.83	66.67	66.67	14.29	17.04
Halloysite	80.00	20.83	50.94	67.48	17.81	ND

ND = not detected.

antimicrobial effect on all tested microorganisms. The microorganisms for which C10A showed the greatest antimicrobial effect were *L. monocytogenes* (30 mm), *E. faecalis* and *S. aureus* (27 mm). Among the test materials, only C10A was found to have an antimicrobial effect on *C. glabrata* (the only yeast species tested), at 18 mm. Compared with the control group, C10A showed greater antimicrobial activity against *P. aeruginosa*. C15A showed an antimicrobial effect only on *S. aureus* (6 mm) and *K. pneumoniae* (15 mm). Halloysite, on the other hand, showed antimicrobial activity against *P. aeruginosa* (10 mm), *E. faecalis* (9 mm) and *S. aureus* (7 mm; Figs 4 & 5 & Table 2).

There have been many studies conducted on the antibacterial properties of natural and chemically modified synthetic clay minerals (Tong *et al.*, 2005; Haydel *et al.*, 2008; Williams *et al.*, 2008). Cerium-loaded halloysite prevents DNA damage, apoptosis, keratosis and abnormal hyperplasia caused by ultraviolet light, thus preventing malignant transformation. It has also been reported that cerium-loaded halloysite prevents biofilm formation by causing oxidative stress to bacterial membranes (Feng *et al.*, 2023b). In addition, gold-loaded halloysite–chitin composite hydrogels have been reported to exhibit high antibacterial activity (Zhao *et al.*, 2023). Today, French clays rich in smectite are used in the treatment of necrotizing fasciitis ulcers, the causative agent of which is *Mycobacterium ulcerans*. Although the mineralogy, crystal size and major element chemistry of the clays used previously are similar, it has been found that they have different antimicrobial properties. Therefore, it is assumed that the reasons for these differences in antibacterial mechanisms are not physical but result from chemical transfers or reactions. Williams & Haydel (2010) demonstrated in their cation-exchange experiments that exchangeable cations play a role in the antibacterial process. They reported that the pH and oxidation state buffered by clay mineral surfaces play key roles in controlling the chemistry of the solutions and the redox-related reactions occurring in the bacterial cell wall. We believe that the antimicrobial effect in this study is due to the alteration and disruption of the cytoplasmic membrane permeability of bacteria. However, as stated previously in the literature (Williams *et al.*, 2008), considering that the clay species used retain metal ions from the environment, the mechanism of antimicrobial action of the clay changes depending on the metal retained.

As a result of the antifungal activity experiments, it was determined that the test substances showed antifungal activity (Table 3).

Except for *F. solani*, C10A was found to be the type of clay with the most effective antifungal activity against the other fungi tested. C10A inhibited the mycelial growth of *T. viride* by 85.32% and that of *T. longibrachiatum* by 85.00%. C15A was the least inhibiting clay type (14.29%) of *N. falciformis* mycelial growth. Halloysite did not have an inhibitory effect on *P. glabrum* mycelial growth. We determined that C15A inhibited the mycelial growth of both *T. viride* and *M. plumbeus* by 66.67% (Figs 6 & 7 & Table 3).

Some researchers have found that natural clay minerals do not show antibacterial action. There are a few reports of clay materials having an antimicrobial effect when antimicrobial agents are added. Yue *et al.* (2019) reported that pure halloysite was ineffective against *Aspergillus niger*, *Penicillium citrinum* and *T. viride*. This suggests that halloysites show biocidal activity only when impregnated with oligodynamic metals (Yue *et al.*, 2019). The clays we used in this study contained metals such as Al, Si, Na, Fe, Ti, Ca, Mg and K, and it can be thought that these metals caused the observed antifungal activity. For example, MMTs carrying cetylpyridinium or modified MMTs with copper and silver ions have bacteriostatic and bactericidal activities (Carcelli *et al.*, 1995; Uchida, 1995; Hu & Xia, 2006; Jo *et al.*, 2007; Wang *et al.*, 2007). Meng *et al.* (2009) prepared a new polydimethyloxane/MMT–chlorhexidine acetate (PDMS/OMMT) nanocomposite film by adding chlorhexidine acetate solution to MMT. The addition of OMMT increased the thermal stability of the composite. In addition, when the antimicrobial activity of PDMS/OMMT was evaluated, it was found that it showed strong activity against *E. coli* and *S. aureus* (Meng *et al.*, 2009). In another study, it was determined that a multifunctional MMT-based composite material containing 5-fluorocytosine, antibacterial metal copper ions and quaternized chitosan showed *in vitro* antibacterial activity against *E. coli*, *S. aureus* and *Candida albicans* (Sun *et al.*, 2019).

In this study, it was determined that the antifungal properties of the organoclays were higher than that of halloysite. The most effective antifungal clay type was determined to be C10A.

https://doi.org/10.1180/clm.2024.1 Published online by Cambridge University Press

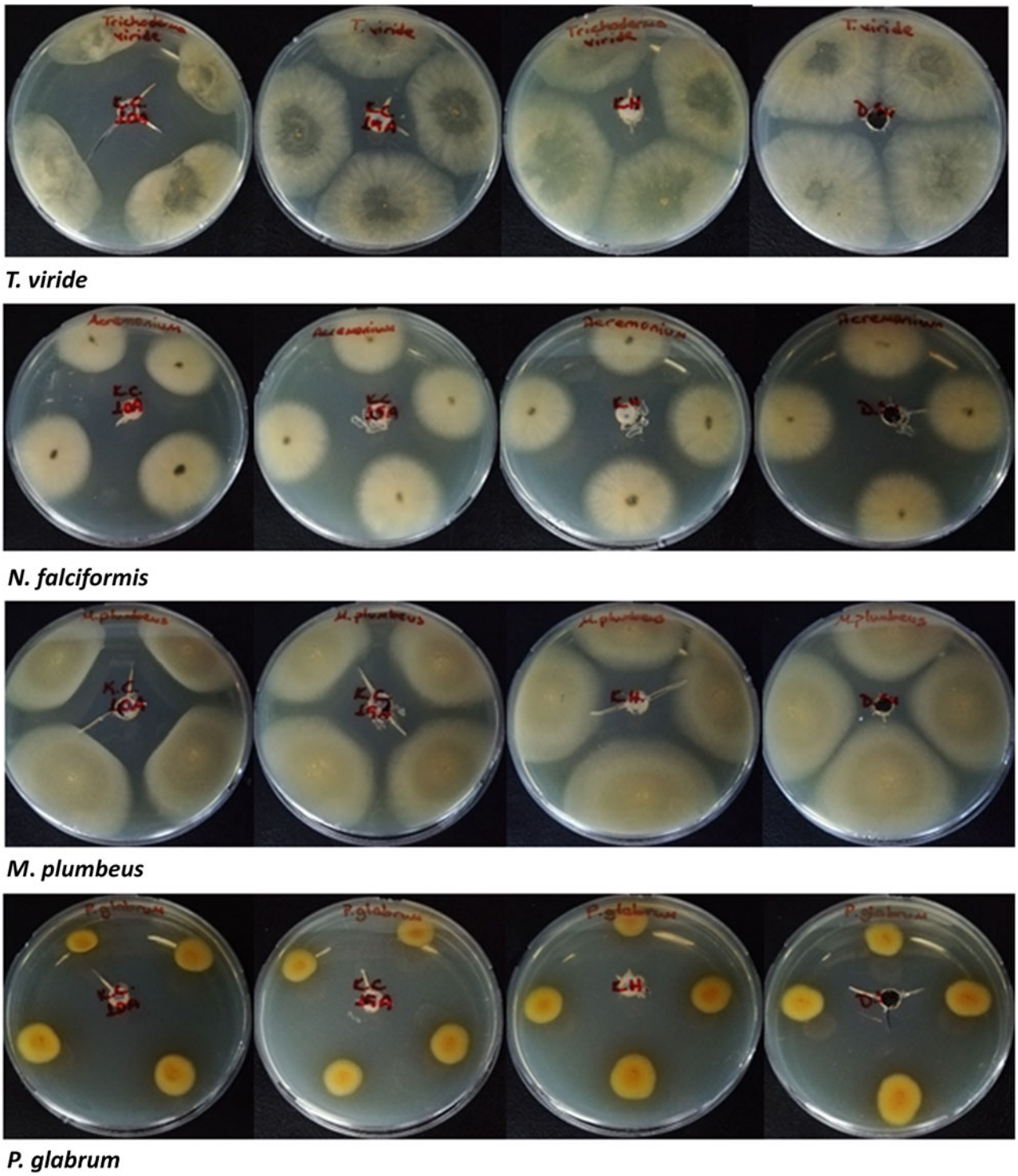

Figure 6. Inhibition of fungal mycelial growth by the studied clays.

Jennings *et al.* (2015) reported that the differences in the antimicrobial activity of QACs are due to the differences in their molecular structure. For example, phenyl (6-phenylnaphthalene) substitution into QACs has been found to significantly increase their antibacterial activity (Zhang *et al.*, 2013; Jennings *et al.*, 2015). The results of this study support the notion that adding a phenyl group to a clay increases its antimicrobial effect, similar to the results of Jennings *et al.* (2015). The ionic interaction of QACs with the bacterial cell membrane disrupts it, allowing proteins, nucleic acids and internal low-molecular-weight materials to flow out, which causes rapid cell lysis (Maillard, 2002; Chapman, 2003; Gilbert & Moore, 2005). The C10A organoclay has a phenyl ring, unlike the C15A organoclay. The QAC sidechains pierce the bacterial intramembrane region as a result of the electrostatic interaction between the positively charged QAC and the negatively charged bacterial cell membrane. This causes

https://doi.org/10.1180/clm.2024.1 Published online by Cambridge University Press

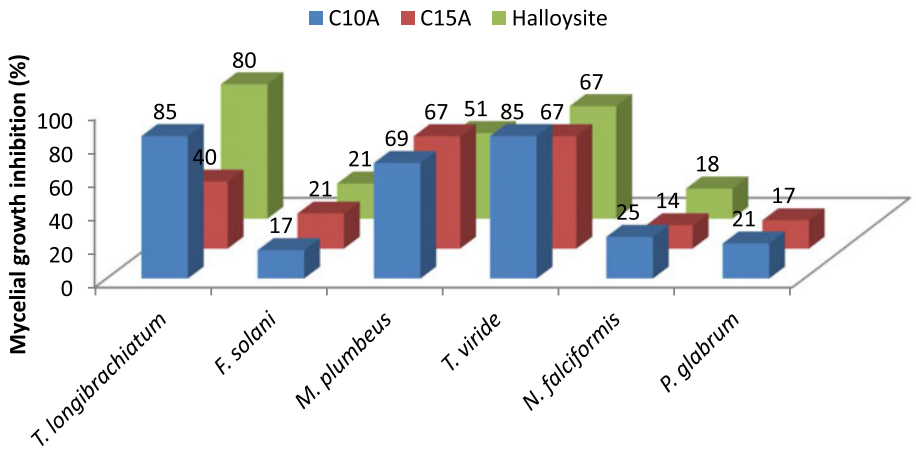

Figure 7. Comparison of the antifungal properties of the studied clays.

Figure 8. Changes of colour after reduction by the studied clays.

cytoplasmic material to leak from the cell and/or the cell to break down (Denyer, 1995).

Although they display notably greater activity against Gram-positive bacteria, QACs can be regarded as broad-spectrum antibiotics due to their ability to affect the bacterial cell membrane. Gram-positive bacteria possess a single phospholipid cell membrane and a thickened peptidoglycan cell wall, whereas Gram-negative bacteria are enclosed by two cell membranes and a relatively thin coating of peptidoglycan. This second membrane means that QACs and other membrane-targeting antiseptics often display an eightfold reduction in activity against Gram-negative pathogens. QACs have also been reported to be potent antifungal agents (Vieira & Carmona-Ribeiro, 2006).

Table 4. DPPH radical-scavenging activities of the studied clays.

Type of clay	Inhibition (%)
C10A	99.90
C15A	99.90
Halloysite	99.64
Control (gallic acid)	99.98

Antioxidant activity test results

When the results of the DPPH experiments were examined, it was determined that the saturated solutions of all test substances presented antioxidant activity (Fig. 8 & Table 4).

Ying (2006) reported that most QACs contain chloride or bromide anions. These structures allow QACs to easily adsorb negatively charged substances (Ying, 2006). Additionally, the inner structure of the HNT is positively charged with Al–OH charges, whereas the outer surface is negatively charged because it contains Si–O–Si bonds (Massaro *et al.*, 2020). This structure causes chemically positively and negatively charged ions to be attached inside or outside the halloysite, respectively. In particular, the positively charged inner surface provides a large area for negatively charged free radicals to attach. However, this adhesion can be increased or reversed by changing the ambient pH and adding different radicals/antioxidants into the system. Therefore, composites with enhanced antimicrobial and antioxidant properties can be formed by adding antioxidants such as ascorbic acid (Baschieri *et al.*, 2019), fatty acids (Lee *et al.*, 2018) or plant extracts (Nastasi *et al.*, 2022) to the structure of the clays (Zhong *et al.*, 2017).

Conclusions

The modified C15A used in this study has two long-chain alkyl groups attached, whereas the modified C10A has a single long-chain alkyl group and a benzyl group attached. It can be said that the differences in the observed antibacterial effect are due to these structures of the molecules. The Cl found in organoclays C10A and C15A and in the quaternary ammonium cations in its structure can be separated from the organoclay by microbial enzymes. Although this causes an increase in antimicrobial activity, the free radicals replacing Cl could contribute to increased antioxidant activity. In addition, it is known that the alkyl chains

https://doi.org/10.1180/clm.2024.1 Published online by Cambridge University Press

and benzyl groups in the structures of QACs have antimicrobial properties. Therefore, more than one mechanism might play a role in the observed antimicrobial effect. Halloysite exhibits antioxidant activity by being positively charged inside the nanotube, interacting with negatively charged ions physicochemically and, as a result, trapping the negatively charged ions inside the tube. Studies conducted by adding various antioxidants to the clay structure found that doing so can increase the antioxidant/antimicrobial activity, helping to more fully explain the underlying antioxidant mechanism. According to these results, organoclays as green source materials could have some applications in industry. For example, antimicrobial polymers are used as additives and coatings in food processing, biomedical devices, filters and antifouling paints. Creating composites by adding the C10A organoclay, which we found to have antimicrobial and antioxidant properties, to plastic materials used in the health, food and biomedical fields can make these materials antiseptic. According to our literature review, this study will provide a significant scientific contribution regarding the antimicrobial and antioxidant properties of C10A, C15A and halloysite. When C10A, C15A and halloysite clays are combined with materials with known antimicrobial and antioxidant properties, these properties can be increased. Future studies should focus on the development of new and effective antimicrobial/antioxidant clay composites.

Conflicts of interest. The authors declare none.

References

Baschieri A., Amorati R., Benelli T., Mazzocchetti L., D'Angelo E. & Valgimigli L. (2019) Enhanced antioxidant activity under biomimetic settings of ascorbic acid included in halloysite nanotubes. *Antioxidants,* **8**, 30.

Biemer J.J. (1973) Antimicrobial susceptibility testing by the Kirby–Bauer disc diffusion method. *Annals of Clinical Laboratory Science*, **3**, 135–140.

Carcelli M., Mazza P., Pelizzi C, Pelizzi G. & Zani F. (1995) Antimicrobial and genotoxic activity of 2,6-diacetylpyridinebis (acylhydrazones) and their complexes with some first transition series metal ions. X-ray crystal structure of a dinuclear copper (II) complex. *Journal of Inorganic Biochemistry*, **57**, 43–62.

Chapman J.S. (2003) Biocide resistance mechanisms. *International Biodeterioration & Biodegradation*. **51**, 133–138.

Chauret C.P. (2014) Sanitization. Pp. 360–364 in: *Encyclopedia of Food Microbiology* (C.A. Batt & M.L. Tortorello, editors). Elsevier, Amsterdam, The Netherlands.

Çankaya N. & Sahın R. (2019) Chitosan/clay bionanocomposites: structural, antibacterial, thermal and swelling properties. *Cellulose Chemistry and Technology*, **53**, 537–549.

Çankaya N., Azarkan S.Y. & Özek N.T. (2021a) Preparation of poly (MPAEMA)/halloysite nanocomposites and investigation of antiproliferative activity. *Journal of the Mexican Chemical Society*, **65**, 189–201.

Çankaya N., Vurgun B. & Yalçın S. (2021b) Antiproliferative effect of organoclay, poly(NCA) and their nanocomposites on HeLa cell line. *Polymer Bulletin*, **78**, 7325–7335.

Denyer S.P. (1995) Mechanisms of action of antibacterial biocides. *International Biodeterioration & Biodegradation*, **36**, 227–245.

Deshmukh R.K., Kumar L. & Gaikwad K.K. (2023) Halloysite nanotubes for food packaging application: a review. *Applied Clay Science*, **234**, 106856.

Ding X., Wang H., Chen W., Liu J. & Zhang Y. (2014) Preparation and antibacterial activity of copper nanoparticle/halloysite nanotube nanocomposites *via* reverse atom transfer radical polymerization. *Royal Society Chemistry*, **4**, 41993–41996.

Duan L., Zhao Q., Liu J. & Zhang Y. (2015) Antibacterial behavior of halloysite nanotubes decorated with copper nanoparticles in a novel mixed matrix membrane for water purification. *Environmental Science: Water Research Technology*, **1**, 874–881.

Feng Y., Luo X., Li Z., Fan X., Wang Y., He R. & Liu M. (2023a) A ferroptosis-targeting ceria anchored halloysite as orally drug delivery system for radiate on colitis therapy. *Nature Communications*, **14**, 5083.

Feng Y., Zhang D., Chen X., Zhou C. & Liu M. (2023b) Confined-synthesis of ceria in tubular nanoclays for UV protection and anti-biofilm application. *Advanced Functional Materials*. Epub ahead of print. DOI: 10.1002/adfm.202307157.

Gilbert P. & Moore L.E. (2005) Cationic antiseptics: diversity of action under a common epithet. *Journal of Applied Microbiology*, **99**, 703–715.

Haiwei J., Hanjun S. & Xiaogang Q. (2016) Antibacterial applications of graphene-based nanomaterials: recent achievements and challenges. *Advanced Drug Delivery*, **105**, 176–189.

Haydel S.E., Remenih C.M. & Williams L.B. (2008) Broad-spectrum *in vitro* antibacterial activities of clay minerals against antibiotic-susceptible and antibiotic-resistant bacterial pathogens. *Journal of Antimicrobial Chemotherapy*, **61**, 353–361.

Hu C.H. & Xia M.S. (2006) Adsorption and antibacterial effect of copper-exchanged montmorillonite on *Escherichia coli* K88. *Applied Clay Science*, **31**, 180–184.

Isik K. & Özdemir-Kocak F. (2009) Antimicrobial activity screening of some sulfonamide derivatives on some *Nocardia* species and isolates. *Microbiological Research*, **164**, 49–58.

Jennings M.C., Minbiole K.P.C. & Wuest W.M. (2015) Quaternary ammonium compounds: an antimicrobial mainstay and platform for innovation to address bacterial resistance. *ACS Infectious Disease*, **1**, 288–303.

Jo S.C., Rim A.R., Park H.J., Yuk H.G. & Lee S.C. (2007) Combined treatment with silver ions and organic acid enhances growth-inhibition of *Escherichia coli* O157:H7. *Food Control*, **18**, 1235–1240.

Kamble R., Ghag M., Gaikawad S. & Panda B.K. (2012) Halloysite nanotubes and applications: a review. *Journal of Advanced Scientific Research*, **3**, 25–29.

Korcan S.E., Kayhan R., Ünal A. & Jahan I. (2021) Determination of antimicrobial effects of western central Anatolian Three Ahlat species. *Afyon Kocatepe University Journal of Sciences and Engineering*, **21**, 250–256.

Kumar L., Deshmukh R.K., Hakim L. & Gaikwad K.K. (2024) Halloysite nanotube as a functional material for active food packaging application: a review. *Food and Bioprocess Technology*, **17**, 33–46.

Lee M.H., Kim S.Y. & Park H.J. (2018) Effect of halloysite nanoclay on the physical, mechanical, and antioxidant properties of chitosan films incorporated with clove essential oil. *Food Hydrocolloids*, **84**, 58–67.

Liu M., Huang J. & Huang M. (2023) The environmental toxicity of halloysite clay and its composites. Pp. 559–574 in: *Clay Composites: Advances in Material Research and Technology* (M. Vithanage, G. Lazzara & A.U. Rajapaksha, editors). Springer, Singapore.

Maillard J.-Y. (2002) Bacterial target sites for biocide action. *Journal of Applied Microbiology*, **92**, 16–27.

Massaro M., Lazzara G, Noto R. & Riela S. (2020). Halloysite nanotubes: a green resource for materials and life sciences. *Rendiconti Lincei. Scienze Fisiche e Naturali*, **31**, 213–221.

Meirelles L.M.A. & Raffin F.N. (2017) Clay and polymer-based composites applied to drug release: a scientific and technological prospection. *Journal of Pharmacy & Pharmaceutical Sciences*, **20**, 115–134.

Meng N., Zhou N.L., Zhang S.Q. & Shen J. (2009) Synthesis and antimicrobial activities of polymer/montmorillonite–chlorhexidine acetate nanocomposite films. *Applied Clay Science*, **42**, 667–670.

Nastasi J.R., Kontogiorgos V., Daygon V.D. & Fitzgerald M.A. (2022) Pectin-based films and coatings with plant extracts as natural preservatives: a systematic review. *Trends in Food Science & Technology*, **120**, 193–211.

Saadat S., Pandey G., Tharmavaram M., Braganza V. & Rowtani D. (2020) Nano-interfacial decoration of halloysite nanotubes for the development of antimicrobial nanocomposites. *Advances in Colloid and Interface Science*, **275**, 102063.

Shchukin D., Price R., Sukhorukov G. & Lvov Y. (2005) Halloysite nanotubes as biomimetic nanoreactors. *Small*, **5**, 510–513.

Shu Z., Yi Z. Ouyyang J. & Yang H. (2017) Characterization and synergetic antibacterial properties of ZnO and CeO_2 supported by halloysite. *Applied Surface Science*, **420**, 833–838.

Silva F.C., Lima L.C.B., Honório L.M.C., Trigueiro P., Osajima J.A., Lobo A.O. & Filho E.C.S. (2019) Clays as biomaterials in controlled drug release: a

scientific and technological short review. *Biomedical Journal of Scientific & Technical Research*, **15**, 11237–11242.

Srivastava A.K. & Dwivedi K.N. (2018) Formulation and characterization of copper nanoparticles using *Nerium odorum* Soland leaf extract and its antimicrobial activity. *International Journal of Drug Development and Research*, **10**, 29–34.

Sun B., Xi Z., Wu F., Song S., Huang X, Chu X. *et al.* (2019) Quaternized chitosan-coated montmorillonite interior antimicrobial metal–antibiotic *in situ* coordination complexation for mixed infections of wounds. *Langmuir*, **35**, 15275–15286.

Tong G., Yulong M., Peng G. & Zirong X. (2005) Antibacterial effects of the Cu(II)-exchanged montmorillonite on *Escherichia coli* K88 and *Salmonella choleraesuis*. *Veterinary Microbiology*, **105**, 113–122.

Uchida M. (1995) Antimicrobial zeolite and its application. *Chemistry & Industry*, **46**, 48–54.

Vieira D.B. & Carmona-Ribeiro A.M. (2006) Cationic lipids and surfactants as antifungal agents: mode of action. *Journal of Antimicrobial Chemotherapy*, **58**, 760–767.

Villano D., Fernandez-Pachon M.S., Moya M.L., Troncoso A.M. & Garcıa-Parrilla M.C. (2007) Radical scavenging ability of polyphenolic compounds towards DPPH free radical. *Talanta*, **7**, 230–235.

Wang J., Li J.X., Ren L., Zhao A.S., Li P., Leng Y.X. *et al.* (2007) Antibacterial activity of silver surface modified polyethylene terephthalate by filtered cathodic vacuum arc method. *Surface and Coatings Technology*, **201**, 6893–6896.

Williams L.B. & Haydel S.E. (2010) Evaluation of the medicinal use of clay minerals as antibacterial agents. *International Geology Review*, **52**, 745–770.

Williams L.B., Haydel S.E., Giese R.F. & Eberl D.D. (2008) Chemical and mineralogical characteristics of French green clays used for healing. *Clays and Clay Minerals*, **56**, 437–452.

Ying G.G. (2006) Fate, behavior and effects of surfactants and their degradation products in the environment. *Environment International*, **32**, 417–431.

Yue X., Yang X., Li H., Zhang R. & Qin D. (2019) Quaternary ammonium compounds-modified halloysite and its antifungal performance. Pp. 121–131 in: *Physics and Techniques of Ceramic and Polymeric Materials* (Y. Han, editor). Springer Proceedings in Physics 216. Springer, Singapore.

Zhang Y., Giurleo D., Parhi, A., Kaul, M., Pilch, D.S. & LaVoie, E.J. (2013) Substituted 1,6-diphenlnaphthalenes as FtsZ-targeting antibacterial agents. *Bioorganic & Medicinal Chemistry Letters*, **23**, 2001–2006.

Zhao P., Feng Y., Zhou Y., Tan C. & Liu M. (2023) Gold@halloysite nanotubes–chitin composite hydrogel with antibacterial and hemostatic activity for wound healing. *Bioactive Materials*, **20**, 355–367.

Zhao X., Wan Q., Fu X., Meng X., Ou X., Zhong R. *et al.* (2019) Toxicity evaluation of one-dimensional nanoparticles using *Caenorhabditis elegans*: a comparative study of halloysite nanotubes and chitin nanocrystals, *ACS Sustainable Chemistry & Engineering*, **7**, 18965–18975.

Zhong B., Lin J., Liu M., Jia Z., Luo Y. & Jia D.F.L. (2017) Preparation of halloysite nanotubes loaded antioxidant and its antioxidative behaviour in natural rubber. *Polymer Degradation & Stability*, **141**, 19–25.

https://doi.org/10.1180/clm.2024.1 Published online by Cambridge University Press